polymer papers

X-ray structure determination of poly(di-n-hexyl silane)

S. S. Patnaik and B. L. Farmer*
Department of Materials Science, University of Virginia, Charlottesville, VA 22903-2442, USA
(Received 5 November 1991; accepted 19 December 1991)

The crystal structure of the low temperature phase of poly(di-n-hexyl silane) (PdnHS) was determined by X-ray diffraction techniques. The backbone chain conformation was found to be all-*trans* and the unit cell to be orthorhombic with dimensions $a = 1.376$, $b = 2.386$ and $c = 0.399$ nm. There are two molecules in a unit cell belonging to the $Pna2_1$ space group. Intermolecular interactions between side chains appear to be predominantly responsible for the all-*trans* backbone. Intramolecular crystallization between the side chains of a molecule does not seem feasible.

(Keywords: crystal structure; low temperature properties; conformation; polysilanes)

INTRODUCTION

Polysilanes are polymers with silicon backbone and hydrocarbon substituents. These polymers with σ-bonded backbone show peak optical absorption in the u.v. region of the spectrum, and many of them exhibit thermochromism and piezochromism. It is believed that these unusual electronic properties of polysilanes result from the σ-electron delocalization along the backbone[1-3] causing their electronic properties to be strongly coupled to the conformation of the silicon backbone. The wavelength of maximum absorption, λ_{max}, seems to be a function of the molecular weight of the polymer and the substituent attached to the silicon backbone. In order to be able to tailor the u.v. absorption, the interdependence of the backbone conformation and the side chain substituents needs to be understood.

Poly(di-n-hexyl silane) (PdnHS), which has two side chains of six methylene units each, is the most studied polymer in the family. In solution, its optical absorption[4] is strongest near 316 nm. The polymer shows reversible thermochromism[2,5,6] and piezochromism[7] in the solid state. Thin films of PdnHS, when heated to 100°C, show maximum absorption at 317 nm (very similar to that seen in solution), shifting to 374 nm on cooling to room temperature. D.s.c. has revealed a strong endotherm (change in enthalpy, $\Delta H = 5.0$ kcal mol^{-1}) at 41°C, which is also associated with the thermochromic transition.

The first order transition at 41°C has been found to correspond to a transition from a three-dimensional crystalline phase at low temperature to a columnar mesomorphic liquid crystalline phase at high temperature[8]. Wide-angle X-ray diffraction patterns indicate that below the transition temperature the polymer is highly crystalline and the backbone has a planar zigzag conformation[9]. In contrast to this, at 60°C (above the transition temperature) a sharp reflection at 1.35 nm (indicative of the polymer interchain spacing) remains, accompanied by a weak equatorial reflection at 0.775 nm and a broad amorphous halo near 0.45 nm with the diffracted intensity concentrated at the meridian[10]. This suggests that, at elevated temperature, the side chains become disordered, but the main chain axes remain parallel and equidistant from each other, and are arranged in a pseudo-hexagonal packing.

The change in the u.v. spectrum with temperature is thought to be associated with a change in polymer backbone conformation, with the long wavelength absorption at low temperature corresponding to a planar *trans* backbone[9,10]. Shifts in λ_{max} with solid state structural changes implies some interdependence of electronic and structural properties. However, the exact origin of these spectral shifts and the nature of these interdependencies are still not clear. Most likely, the planar backbone conformation aids the σ-electron delocalization along the backbone[11], and λ_{max} blue shifts with an increase in temperature as the molecule acquires (presumably) a helical conformation allowed by side chain disordering.

It has been proposed that at low temperature, side chain crystallization forces the backbone to be all-*trans*[9,11]. Alternatively, intermolecular interactions may be responsible for forcing the backbone into an all-*trans* conformation even if the lowest energy form for an individual molecule is a helical conformation (molecular mechanics calculations for single chains have found a 7/3 helix to be of the lowest energy[12]).

The crystal structure of PdnHS has to be determined in order for the nature of the driving force to be understood. Though PdnHS is known to have an all-*trans* backbone at room temperature, little is known about the conformation of the side chains and the crystal packing. In this paper, the crystal structure of PdnHS is discussed as determined by X-ray diffraction techniques.

* To whom correspondence should be addressed

0032-3861/92/214443-08

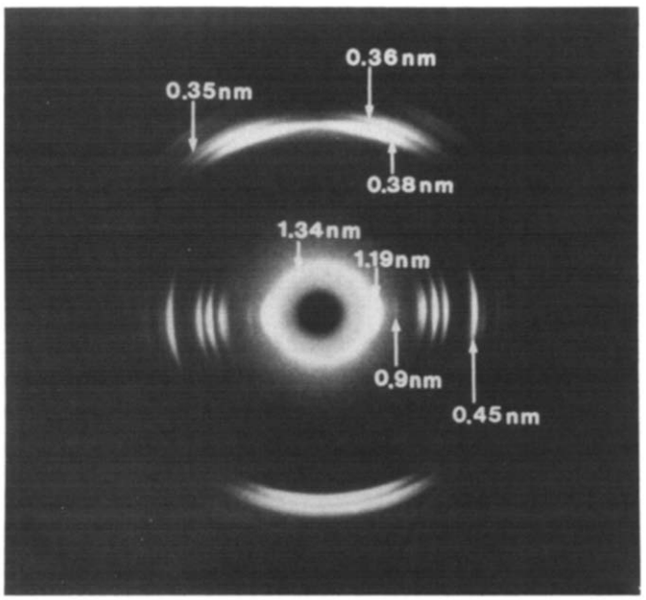

Figure 1 Wide-angle X-ray diffraction pattern of oriented PdnHS obtained at room temperature

EXPERIMENTAL

X-ray measurements

Wide-angle fibre diffraction patterns were recorded using nickel-filtered CuKα radiation. Oriented fibres of the sample were mounted with the fibre axis parallel to the camera axis and perpendicular to the X-ray beam. A flat plate camera was used to record the low-angle reflections and a cylindrical camera of 57.3 mm radius with pinhole collimation was used to record the large-angle reflections. Optical density data were collected from the photographically recorded X-ray diffraction pattern (*Figure 1*) using a two-dimensional scanning microdensitometer. The data were first corrected for film response characteristics. The background correction was then made by taking a small area in the corner of the pattern as representative of the background intensity. To make further corrections, the origin of the film coordinate system had to be located, so the centre of the pattern was determined by selecting two equivalent reflections from either side of the equator and using a computer program to find a point equidistant from them on the equator. Fibre tilt was corrected by using another program[13]. These data were further corrected for contributions from Lorentz and polarization factors. Reflections on the zero and the first layer lines were measured and the reciprocal lattice coordinates corresponding to the position on the film were calculated[14]. Reflections out to 0.3 nm on the zero layer line could be measured using the film from the flat plate camera. To record the intensities of the higher angle reflections, the cylindrical camera had to be used and the exposure time increased. This resulted in saturating the low-angle, strong reflections. Using the cylindrical camera, reflections out to 0.2 nm were observed and the intensities were scaled with respect to those measured from the flat camera.

Unit cell determination

The *d*-spacings calculated from powder diffractometer scans are more reliable than those measured from the films; therefore, powder diffraction data were also recorded using a Scintag θ–θ diffractometer. These *d*-spacings (*Table 1*) were used for the unit cell refinement. Corresponding to each low-angle reflection measured by the diffractometer, a reflection was seen on the zero layer line of the fibre pattern, and the *d*-spacings measured from the film agreed within 3% with those from the diffractometer measurements.

At room temperature, Lovinger *et al.*[10] reported the presence of a second phase (the high temperature phase) along with the crystalline low temperature phase. They attributed the strong peak at 1.35 nm to this high temperature phase. Our fibre diffraction pattern showed a corresponding intense ring at 1.34 nm which, unlike the other reflections, exhibited no preferred orientation. This confirmed that it indeed is due to a second phase, and the reflection was not considered in the subsequent refinement of the unit cell.

Using the reflections indexed as zero layer reflections, an orthorhombic unit cell of $a = 1.376$ and $b = 2.386$ nm was found from the powder diffraction data. The average discrepancies in the *d* values (Δd), and the diffraction angles ($\Delta 2\theta$) were 0.0007 nm and 0.05°, respectively. Two slightly different layer line spacings have been reported: 0.407 nm by Kuzmany *et al.*[9] and 0.40 nm by Lovinger *et al.*[10]. Since the *d*-spacings used from the diffractometer scan could be indexed by zero layer reflections, the present unit cell refinement did not address the layer line spacings. Measurement of the layer line spacing from fibre diffraction patterns after correction for the fibre tilt,

Table 1 Powder diffraction data of PdnHS

d_{obs} (nm)	d_{cal} (nm)	*hkl*
1.344[a]		
1.191	1.193	020
	1.192	110
0.900	0.901	120
0.688	0.688	130
	0.688	200
0.660	0.661	210
0.560	0.596	040
	0.596	220
0.549	0.547	140
0.452	0.451	150
	0.451	240
	0.450	310
0.428	0.428	320
0.398	0.398	060
	0.398	330
0.384	0.382	160
0.364	0.364	340
0.345	0.344	260
	0.344	400
0.332	0.331	170
	0.331	350
	0.330	420
0.300	0.300	360
	0.298	440
	0.298	080
0.275	0.274	280
0.261	0.260	190
	0.260	460
	0.260	530
0.250	0.250	540
0.239	0.239	0100
0.221	0.220	630
0.215	0.214	1110
	0.214	570
	0.214	640

[a] Due to phase II, not included in unit cell refinement

Table 2 First layer line reflections

d_{obs} (nm)	d_{cal} (nm)	*hkl*
0.384	0.394	0 1 1
	0.384	1 0 1
	0.379	1 1 1
0.364	0.366	1 2 1
0.355	0.357	0 3 1
	0.346	1 3 1
	0.342	2 1 1
0.330	0.332	2 2 1
0.304	0.306	0 5 1
	0.301	3 0 1
0.284	0.282	3 3 1
	0.280	2 5 1
0.260	0.261	2 6 1
	0.259	0 7 1
	0.259	4 1 1

yielded an average value of 0.399 nm, so a *c* axis of 0.399 nm was chosen. The earlier reported value[9] of 0.407 nm falls within the experimental error. In order to match the experimentally measured density[15] of 0.929 g cm^{-3}, the X-ray unit cell must have two molecules. The density of the 100% crystalline polymer calculated from the X-ray unit cell volume was 1.004 g cm^{-3}.

Reflections from the first layer line are given in *Table 2*. The observed *d*-spacings are those measured using a diffractometer. No reflections could be found on the powder diffractometer scan corresponding to the two reflections on the film at 0.355 and 0.284 nm, so their reported *d*-spacings were calculated from the average of three independent measurements from the film. The diffraction patterns from the flat film camera showed that these reflections were broader than those on the zero layer line. Thus, there was less accuracy in the *d*-spacing measurement of these two reflections compared to the *d*-spacings of the other reflections (which were measured from the diffractometer scan). The reflections at 0.384, 0.364 and 0.355 nm overlapped so their individual intensities could not be accurately measured and they had to be considered as a composite spot. A reflection at 0.412 nm was present in the fibre and powder diffraction patterns reported by Kuzmany *et al.*[9], and was the only reflection that could not be then indexed by an orthorhombic unit cell. This reflection was absent in the diffractometer scan from the same sample taken 2 years later. Thus, an orthorhombic unit cell was used for further refinement.

SPACE GROUP DETERMINATION

For an orthorhombic crystal system, there are three possible point groups: 222, *mm*2 and *mmm*. The *mmm* point group requires a mirror plane perpendicular to the *c* (molecular) axis. The only way a mirror plane can be placed normal to the molecular axis in PdnHS is with the two hexyl side chains attached to the same silicon atom, arranged on a plane normal to the backbone axis. This seems extremely unlikely because it would lead to excessive intramolecular steric crowding (molecular mechanics calculations have shown that the side chains have to be non-orthogonal to the backbone axis in order to relieve intramolecular steric crowding[12]). The two more likely point groups are thus *mm*2 and 222. Various space groups based on these two point groups were considered.

Since it is known that the polymer backbone has an all-*trans* conformation, a unit cell with *c* repeat of 0.399 nm can accommodate only two consecutive silicon atoms. The density measurements showed that there are two molecules per unit cell, so there must be four silicon atoms per unit cell. The symmetry of the possible space groups requires that each silicon atom occupy one of the four equivalent positions.

From examination of the Miller indices of the observed reflections (*Tables 1* and *2*), no systematic absences were apparent. Since a centred lattice would have systematic extinctions throughout reciprocal space, a side-centred, face-centred or body-centred lattice could be ruled out, i.e. only primitive space groups needed to be considered. The point group *mm*2 gives rise to 10 primitive space groups and the point group 222 gives rise to 4 primitive space groups. Of these, only two, $Pca2_1$ and $Pna2_1$, have equivalent positions such that four silicon atoms with two atoms displaced from the other two by 1/2*c* can be placed in them. Thus, the remaining potential candidates were $Pna2_1$ and $Pca2_1$.

ELECTRON DENSITY MAPPING

Though there were not enough reflections to accurately determine the positions of atoms using electron density maps, an attempt was made to use these maps to choose between the two possible space groups. To calculate the electron density map, an initial estimate of the positions of atoms is required. Once the position of the molecular axis in the unit cell is fixed, for a given backbone torsion angle and bond angle, the position of the first carbon atoms of the side chains can be determined from geometry. Since nothing more was known about the rest of the side chain at this point, a model consisting of two silicon atoms per molecule and the attached first carbon atoms was considered.

To determine the position of the molecular axis, two-dimensional electron density maps were calculated using the zero layer reflections. $Pca2_1$ requires one molecule to be at the corner and the second to be midway along the *a* or *b* axis, while $Pna2_1$ requires one at the corner and the other at the centre of the unit cell. Therefore, the following three cases were considered: case 1, molecular axes at (0,0,0) and (1/2,0,0); case 2, axes at (0,0,0) and (0,1/2,0); case 3, axes at (0,0,0) and (1/2,1/2,0). For each case the fractional coordinates of the atoms were calculated. Using these positions, the amplitudes and phases of the structure factors of the observed reflections were calculated. These calculated phases were then used with the observed structure factor amplitudes to produce the electron density maps. If indeed the input positions of the atoms were correct, the electron density map should show regions of high electron density around the input positions.

To generate the electron density map, a grid of 0.03 nm was used. In the first two cases, although a high electron density area was seen at the corner, the position of the second molecule could not be located. The $Pca2_1$ space group was thus rejected. The third case showed two regions of highest electron density (at the corner and in the middle) and a band of high electron density along the diagonal (110). Different orientations of the molecules for case 3 were examined. In each case the electron density was found to be high along the diagonal. The number of reflections is not sufficient and the resolution of data

not good enough to make any further determination of the orientation of the molecules based on the electron density maps.

STRUCTURE REFINEMENT METHOD

The structure was refined using the structure refinement computer program LALS (linked-atom least-squares) which has been developed by Smith and Arnott[16]. Least squares refinement of the observed diffraction data cannot be used successfully to refine a structure unless the number of observed reflections is significantly larger than the number of parameters being varied. To refine individual atomic positions, the number of reflections should be at least six times the number of atoms. In polymers this is seldom the case. Therefore, it is necessary to reduce the number of independent variables. LALS overcomes this limitation by considering the molecule as a linked atom system and by supplementing fibre diffraction data with stereochemical information. The position of each atom is defined in relation to the previous atoms by a bond length, a bond angle and a torsion angle. The molecular and crystal models are then refined so that the calculated structure factors best fit the observed structure factors and so that the molecule is stereochemically reasonable (e.g. the model exhibits no excessively short non-bonded contacts). LALS allows the refinement of bond angles, torsion angles, intermolecular packing parameters, scale factor and isotropic temperature factor. By keeping the bond lengths and angles fixed (as in our case), the determination of polymer structure is reduced to determining the torsion angles about bonds and the orientations and the positions of the molecules in the unit cell.

Structure refinement proceeds by refining various defined parameters in order to minimize the weighted R factor (R'')

$$R'' = \left(\frac{\sum_i W_i |F_{obs} - F_{cal}|_i^2}{\sum_i W_i |F_{obs}|_i^2} \right)^{1/2} \times 100$$

where W_i is the weight attached to the observation of the ith reflection. Ideally, W_i should be given a value proportional to the variance of the value of the ith reflection, but in practice all W_i are usually chosen to be equal for all reflections. The more commonly reported, conventional R factor, defined by

$$R = \frac{\sum_i |F_{obs} - F_{cal}|_i}{\sum_i |F_{obs}|_i} \times 100$$

is also reported.

STRUCTURE REFINEMENT

The PdnHS molecule was described as a 2_1 helix, with the helix axis along c. Two molecules per unit cell were considered with one at the corner and the other at the centre. The bond lengths and angles used are given in *Table 3*. The Si–Si–Si bond angle of 116.2° was chosen based on X-ray diffraction data (all-*trans* backbone with fibre repeat of 0.399 nm) and Si–Si bond length of 0.235 nm.

Table 3 Bond lengths and angles

	Bond length (nm)		Bond angle (deg)
Si–Si	0.235	Si–Si–Si	116.2
Si–C	0.188	Si–Si–C	107.7
C–C	0.153	Si–C–C	114.0
C–H	0.109	Si–C–H	108.3
		C–C–H	109.1
		C–C–C	111.0

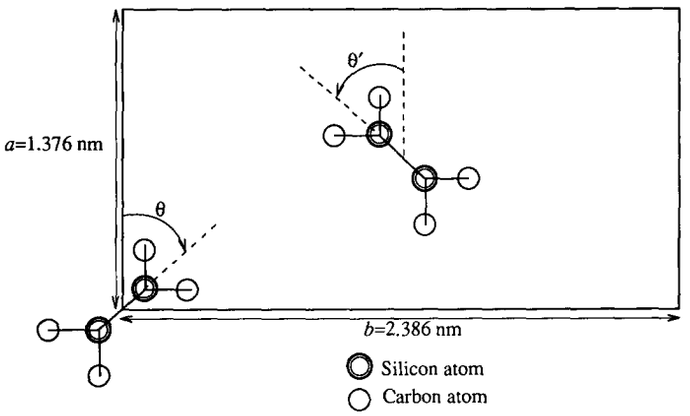

Figure 2 Schematic representation of the initial unit cell model

For the structure refinement, intensities measured using the flat camera were used. The extra (higher angle) reflections observed using the cylindrical camera, were used to check the model by comparing the calculated and observed intensities and addressing unusual discrepancies. The two very strong reflections, at 1.191 nm on the zero layer line and the off-meridional composite reflection on the first layer line, were not considered numerically in the refinement due to the inaccuracy in measuring their intensities. Both of these reflections overlap with reflections due to phase II. The diffraction pattern (*Figure 1*) shows that the reflection at 1.191 nm overlaps with the intense ring (at 1.34 nm) attributed to phase II. Since this phase II reflection is so sharp at room temperature, it is very likely that the amorphous halo due to phase II, with its intensity concentrated at the meridian[10], is also present and overlaps the off-meridional first layer line reflections (at 0.384, 0.364 and 0.355 nm). This can account for the very broad nature of the off-meridional first layer reflections. The reflection at 0.9 nm on the zero layer line was given half weight because it is very close to the thick ring due to phase II, and seems to have an abnormally high background intensity.

An initial model (*Figure 2*), like the one used for electron density mapping, was refined against the zero layer reflections first. The two molecules were rotated independently in steps of 10°, and for each setting of the molecular axis, the R factor was calculated by refining the scale and the isotropic temperature factors. Many low R factor settings were located, of which two settings—orientation I ($\theta = 20°$, $\theta' = -20°$) and orientation II ($\theta = 30°$, $\theta' = -30°$)—are allowed by the space group $Pna2_1$ (the symmetry of the space group requires $\theta = -\theta'$). The rest of the side chain atoms were included in the model at this point with torsion angles initially considered to be *trans*. For both cases (orientations I and II), torsion about the C_1–C_2 bond on each side chain was changed in 10° steps and the corresponding R factor calculated. The lowest R factor was found for orientation I ($\theta = 20°$) and the torsion angle about the C_1–C_2 bond equal to 50.0° (*trans* being defined as 180°).

Table 4 Internal rotation angles after refining against zero layer reflections

Torsion angle	Value (deg)[a]
$Si_1(1)$–$Si_2(2)$–$C_1(3)$–$C_2(4)$ (τ_1)[b]	30
$Si_2(2)$–$C_1(3)$–$C_2(4)$–$C_3(5)$ (τ_2)	173
$C_1(3)$–$C_2(4)$–$C_3(5)$–$C_4(6)$ (τ_3)	148
$C_2(4)$–$C_3(5)$–$C_4(6)$–$C_5(7)$ (τ_4)	−178
$C_3(5)$–$C_4(6)$–$C_5(7)$–$C_6(8)$ (τ_5)	154

[a] All-*trans* conformation is defined to be 180°
[b] Numbering of atoms is shown in *Figure 3*

Table 5 Final internal rotation angles

Torsion angle	Value (deg)[a]
$Si_1(1)$–$Si_2(2)$–$C_1(3)$–$C_2(4)$ (τ_1)	30
$Si_2(2)$–$C_1(3)$–$C_2(4)$–$C_3(5)$ (τ_2)	173
$C_1(3)$–$C_2(4)$–$C_3(5)$–$C_4(6)$ (τ_3)	142
$C_2(4)$–$C_3(5)$–$C_4(6)$–$C_5(7)$ (τ_4)	−179
$C_3(5)$–$C_4(6)$–$C_5(7)$–$C_6(8)$ (τ_5)	156

This was the initial geometry of the molecule considered for refinement. The initial torsion angles were $\tau_1 = -\tau_1' = 50°$, $\tau_2 = -\tau_2' = 180°$, $\tau_3 = -\tau_3' = 180°$, $\tau_4 = -\tau_4' = 180°$ and $\tau_5 = -\tau_5' = 180°$, where τ_x and τ_x' are the corresponding torsion angles in the two side chains attached to the same silicon atom (the torsion angles are defined in *Tables 4* and *5*). Energy calculations on isolated molecules having an all-*trans* backbone found two side chain conformations to be of low energy: the side chains normal to the backbone and extending roughly parallel to the plane formed by the silicon atoms in the all-*trans* backbone; and the side chains normal to the backbone and extending roughly normal to the plane formed by the silicon atoms in the all-*trans* backbone[17]. The starting X-ray model is closer to the former, which also has the lower energy.

The two molecules in the unit cell—one at the corner and the other at the centre—were oriented at $\theta = 20°$ and $\theta' = -20°$, respectively, and, as required by the space group, their geometry was considered to be the same (i.e. molecules 1 and 2 are exactly the same except for the setting angles). The model was refined by varying the five side chain torsion angles τ_1, τ_2, τ_3, τ_4 and τ_5, and the scale and temperature factors, with the corresponding torsion angles on the two side chains constrained to be of equal magnitude, i.e. $\tau_x = -\tau_x'$, etc. Letting the two side chains attached to the same silicon atom have different torsion angles did reduce the R factor further, and also reduced the number of contacts. However, decreasing the R factor by increasing the number of variables does not necessarily mean that the model is better. In our case, the decrease in R is not statistically significant, and does not justify a two-fold increase in the degrees of freedom. In addition, with the limited number of reflections, the data-to-parameter ratio decreases to the point that the refinement is no longer meaningful. The side chains attached to the same silicon atom were thus considered to be mirror images of each other (*Figure 3*). The internal rotation angles after refinement against zero layer reflections are given in *Table 4*. The corresponding residuals were found to be $R = 11.6$ and $R'' = 14.4$.

Next, both the zero and the first layer line reflections were included in the refinement and the side chain torsion angles were again refined. The refined torsion angles are given in *Table 5*. The residuals for this structure (*Figure 3*) were $R = 13.8$ and $R'' = 13.3$. For comparison purposes the maximum R factor[18,19], R_{max}, which is the residual for a model with the same symmetry as the correct model but with an unrelated arrangement of atoms is 52.0. The average uncertainty associated with the refined torsion angles, given in *Tables 4* and *5*, is $\sim 1.5°$. However, it is expected that the outer torsion angles will have larger uncertainties than those closer to the backbone. This estimate of the uncertainties should not be considered a well defined mathematical quantity, and has been included here to give an indication of the variation that can be seen in the values of the torsion angles without seriously affecting either the R factor or the number of non-bonded contacts. Comparing *Tables 4* and *5*, it is clear that, except for τ_3, the changes in torsion angles are within the uncertainty limit. Thus, the only torsion angle significantly affected by the first layer reflections was τ_3. Although changing the relative z coordinates of the two molecules in the unit cell is not allowed by the space group symmetry, such translations were considered. However, shifting the molecule in the centre of the unit cell along the z axis with respect to the one at the corner increased the R factor.

Table 6 lists the observed and calculated structure factor amplitudes of the observed reflections. The listed planes are those from *Tables 1* and *2* whose calculated structure factors best fit the observed structure factors. As mentioned earlier, the two very strong reflections were not considered numerically in the structure refinement. However, their calculated structure factors were greater than that of any other reflections, in agreement with experiment. Unobserved reflections are those reflections which are too weak to be observed against the background intensity. If the model is correct, experimentally

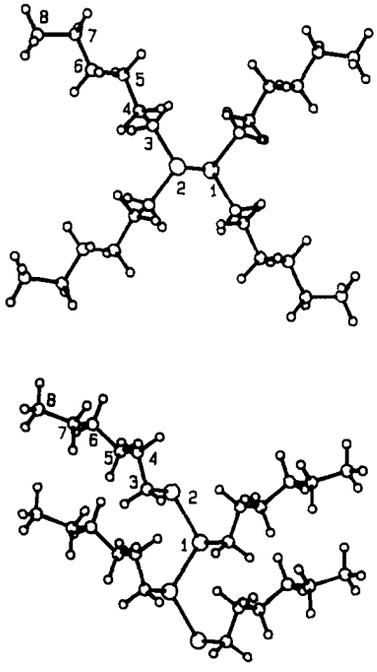

Figure 3 Ball and stick representation of the PdnHS molecule. The large circles represent silicon atoms, the medium circles represent carbon atoms and the small circles represent hydrogen atoms. The top figure shows the *ab* projection and the bottom figure shows the molecule along the c (chain) axis

Table 6 Comparison between observed and calculated structure factor amplitude[a]

hkl	$\|F_{obs}\|$	$\|F_{calc}\|$
110,020	Very strong	110
120[b]	46	20
130,200	50	45
210	78	84
220,040	104	96
140	89	92
150	100	95
320	56	65
330	43	49
160	39	38
260	22	32
170	28	33
440	17	22
031,211,121 } 111,131,201 }	Very strong	108
221	62	55
051	30	22
331	32	39
401,411,071,261	40	34

[a] In case of overlapping reflections contributing to the intensity of a spot, the planes are listed in order of decreasing intensity. The observed structure factor amplitude $|F_{obs}|$ is equal to $k(I_{obs})^{1/2}$, where I_{obs} is the observed relative intensity and k is the scale factor. The calculated structure factor amplitude $|F_{cal}|$ is equal to $(mF_c^2)^{1/2}$, where m is the multiplicity and F_c is the calculated structure factor of single planes. For overlapping reflections this value is $(\sum mF_c^2)^{1/2}$

[b] Weight used as 0.5

unobserved reflections should not have high calculated intensities. For our model, the structure factors corresponding to all possible reflections were calculated, and the strongest unobserved reflection was found to have a calculated intensity comparable to the weakest observed reflection.

The structure factors were computed with a refined overall isotropic temperature factor of 0.2 nm^2. The refined scale factor was 2.17. These two quantities have an estimated uncertainty of 0.001 nm^2 and 0.3%, respectively. A temperature factor of 0.2 nm^2, though quite high, is not uncommon for polymers[20]. It has been reported that the side chains of PdnHS are partially crystalline, and above the glass transition temperature (−52.5°C), two CH_2 groups in each side chain are mobile[21]. These mobile CH_2 groups would then have high temperature factors associated with them. Since LALS does not have a provision for calculating temperature factors for individual atoms, these mobile CH_2 groups contribute to the high isotropic temperature factor.

Along with the diffraction data, LALS uses overly short interatomic distances between non-bonded atoms in the least-squares optimization. The effect of choosing different values of allowed contact distances was also studied. Since the main contribution to the steric interaction in PdnHS comes from non-bonded interactions between the side chains, two sets of contact distances with different C–C, C–H and H–H non-bonded distances were considered: case I, with the closest distance of approach between two atoms being slightly smaller than the sum of their van der Waals radii[22] (as observed in certain molecular crystals), and case II, with the allowed contact distances between two atoms equal to the sum of their van der Waals radii plus 0.02 nm (ref. 16). The Si–Si contact distance was taken to be 0.36 nm. No significant difference in the structure refinement was noticed while using the different sets of contact distances, and the values from case I were used in the final refinement. No short intermolecular contacts were found. The closest contact between carbon atoms of the same molecule was 0.02 nm short of the allowed value and was relatively insignificant. The worst intrachain contact was between the hydrogen atoms attached to carbon atoms on successive side chains. It was found to be 0.05 nm short of the allowed value, and was much more significant. However, due to the limited number of X-ray reflections, the bond angles were kept constant in this refinement, and only the torsion angles could be varied. The close contacts would be relieved if the bond angles and bond lengths were also allowed to vary.

DISCUSSION

The low temperature crystalline phase of PdnHS was found to be orthorhombic with unit cell dimensions $a=1.376$, $b=2.386$ and $c=0.399$ nm. The unit cell dimensions are such that the crystal lattice (*Figure 4*) can be considered pseudo-hexagonal, i.e. the molecular chain axes are arranged in an almost hexagonal lattice but the molecules themselves do not have hexagonal symmetry. This is not surprising since hexagonal packing is commonly observed for polymers with long alkane side chains[23,24]. At temperatures above the transition temperature, with the disordering of side chains and the backbone, the molecule acquires a cylindrical rod-like shape and packs in a hexagonal arrangement[8,11]. It can be seen from *Figure 4* how the molecules in the low temperature phase might easily arrange themselves in a hexagonal lattice without much axial displacement.

The side chain torsion angles (*Figure 3*) are such that, in projection along the molecular axis, the molecule looks very similar to the one found to have the lowest energy[17].

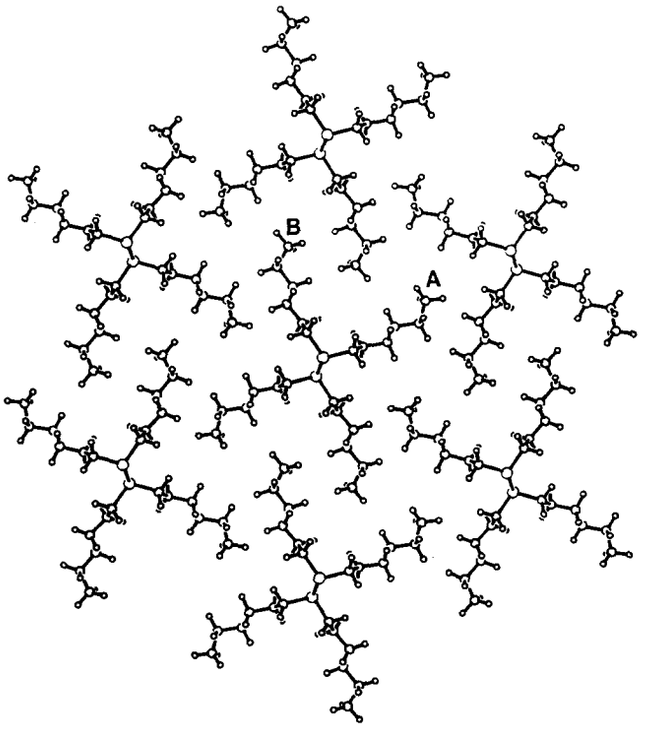

Figure 4 Projection of the PdnHS crystal lattice on the *ab* plane. The medium circles represent carbon atoms and the small circles represent hydrogen atoms

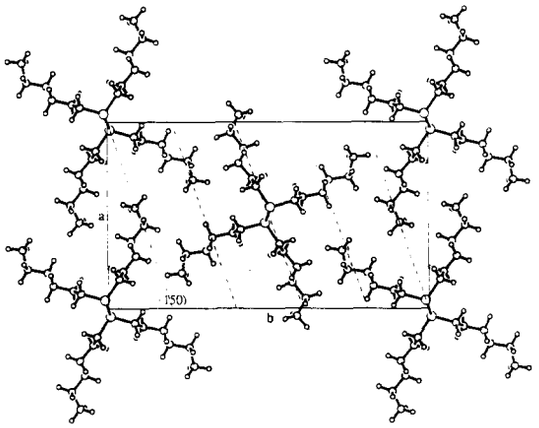

Figure 5 Projection of the orthorhombic PdnHS unit cell on the *ab* plane. The broken lines show {150} planes

The X-ray analysis shows (*Figure 3*) that the side chains are not normal to the backbone, supporting the earlier findings of Kuzmany *et al.*[9]. We observe two almost-*trans* bonds (τ_2 and τ_4) and no *gauche* bonds in the side chains. Both of these observations are consistent with results from the Fourier transform-Raman spectroscopic studies of Hallmark *et al.*[25]. The hexyl side chains, being attached at one end to the silicon backbone, can no longer pack efficiently as all-*trans* alkane segments (found for n-alkanes), and non-*trans* torsions are introduced, perhaps to generate a more space filling, higher density crystal structure.

Figure 4 shows that the side chains are arranged such that the molecules are closely packed. The unexpectedly large gap around the edge of the side chains is consistent with the large temperature factor found for the molecule. In the case of alkoxycinnamic acids, it has been found that for the temperature factor increasing from 0.08 to 0.3 nm^2, the thermal ellipsoid can increase by as much as four times[26]. Thus, if the outer methylene units in the side chain of the PdnHS molecule are more mobile than the methylene groups closer to the backbone, and are largely responsible for the temperature factor of 0.2 nm^2, their thermal ellipsoids will also be larger and will result in filling the large gap.

The two side chains A and B (see *Figure 4*) attached to the same silicon atom see somewhat different local intermolecular environments. This could give rise to the splitting of the carbon resonances into approximate 1:1 doublets as found by ^{13}C cross-polarization/magic angle spinning n.m.r. studies[27,28]. The splitting of methyl and methylene carbon resonances in some polymer systems has been explained as being due to the presence of different local packings[29]. Schilling *et al.*[30] have attributed the splitting in PdnHS to the possibility of two slightly different side chain packings (very small chemical shifts have likewise been reported in the literature for alternative modes of packing in n-alkanes[31]).

It has been suggested[10,11,25] that the 0.452 nm reflection is characteristic of the packing of *trans*-planar alkyl side chains into a triclinic unit cell (found for n-hexane, n-heptane and n-octane). Our results show that the side chains are not completely *trans*-planar (*Table 5*, also see *Figure 3*), so any comparison with *trans*-planar alkane packing is inappropriate. Since the side chains are not completely *trans*-planar, and also not normal to the backbone (*Figure 3*), it is difficult to see how the side chains from adjacent silicon chains can pack into alkyl sheets parallel to the silicon backbone direction, as suggested by Lovinger *et al.*[10]. However, the 0.452 nm reflection corresponds to the 150 planes (*Figure 5*), which can be seen to contain one set of the side chains. Thus, the reflection could, in some ways, be considered as representative of the packing of one set of the side chains in projection, although the Si–Si planes also contribute to the reflection. As can also be seen from *Figure 5*, the other set of side chains is along the 110 direction, rendering it also very strong.

It has been proposed that side chain crystallization forces the silicon backbone into an all-*trans* conformation[11]. Though side chain crystallization implies crystallization between side chains of neighbouring molecules, the use of the term 'side chain crystallization' in the literature in the present context has been ambiguous. A distinction needs to be made between crystallization of the side chains of the neighbouring molecules and that between side chains of the same molecule. The term 'side chain crystallization' is mostly used for polymers that have very low crystallinity (30%), where the side chains arrange themselves in small crystallites but the polymer backbone remains in the amorphous phase. In the present case the polymer is ~60% crystalline[21] and very highly ordered within the crystals. The backbone is obviously participating in the crystallization, so it does not seem appropriate to differentiate between side chain and overall crystallization. It is clear from *Figure 4* that the structure adopted by each molecule is such as to minimize the interactions between its own side chains. Thus, intramolecular side chain crystallization can certainly be ruled out.

A question that still remains is, does intermolecular side chain crystallization occur? It is not obvious from *Figure 4* that the side chains find themselves in an environment which is dramatically preferable or unique and, therefore, merits such a characterization as 'side chain crystallization'. It is apparent however, that reducing the length of the side chains would decrease the intermolecular side chain interactions and make the all-*trans* structure less favourable, perhaps accounting for the helical structures of poly(di-n-pentyl silane) and poly(di-n-butyl silane). Similarly, the structures are not very efficiently packed so that increasing the lengths of the side chains would also make the all-*trans* structure less favourable. It is expected that for poly(di-n-alkyl silanes) with longer side chains, side chain crystallization is very likely to be present. Side chain crystallization is found for polymers with long alkyl side chains[23,24,32]. X-ray results indicate that poly(n-alkyl acrylates), poly(n-alkyl methacrylates) and poly(vinyl ethers) with 10 or more carbon atoms in their side chains are crystalline and the crystallites are made up of segments of the side chains. Similar to what is observed for paraffin hydrocarbons, these polymers show a sharp X-ray diffraction ring at 4.2 Å, suggesting that the long side chains pack into paraffin-like crystallites.

The molecules are packed in a closest packing crystal structure (the $Pna2_1$ space group allows closest packing[33]). Therefore, the side chains of neighbouring molecules certainly influence each other, and their interactions must affect the backbone conformation. Molecular mechanics calculations on isolated PdnHS molecules, which consider only intramolecular interactions, found a 7/3 helical conformation to be of lowest

energy[12]. If intramolecular interactions were indeed the dominant interactions in determining the backbone structure, then the energy calculations would have found the observed all-*trans* conformation to be of lowest energy. This suggests that intermolecular, not intramolecular, forces play a dominant role in determining the crystal structure. Crystal packing calculations should be carried out to determine the packing energy of all-*trans* and the 7/3 helical conformations and to determine the lowest energy conformation in the solid state. It is expected that the crystal packing energy of the all-*trans* conformation, as found by our X-ray analysis, will be lower than that of the 7/3 helical conformation. That such intermolecular influences may be effective in stabilizing the backbone conformation is indicated by calculations on poly(dimethyl silane) (PdMS). For PdMS it has been found that the packing energy of the all-*trans* backbone molecule is lower than that of the 15/7 helix, although an isolated all-*trans* molecule has higher energy than an isolated 15/7 helix[34].

CONCLUSIONS

The crystal structure of the low temperature phase of PdnHS has been determined. The unit cell was found to be orthorhombic with dimensions $a=1.376$, $b=2.386$ and $c=0.399$ nm, and the space group was determined to be $Pna2_1$. Although the backbone conformation of PdnHS is all-*trans*, the alkyl side chains are not completely all-*trans*. The side chains are not normal to the backbone. They extend roughly parallel to the plane formed by the silicon backbone. The corresponding conventional *R* factor for this structure was found to be 13.8. The presence of the all-*trans* backbone conformation which was earlier determined to be not of lowest energy for an isolated molecule[12], and the arrangement of the side chains which appear to minimize intramolecular interactions, indicate that intermolecular interactions are primarily responsible for stabilizing the all-*trans* backbone conformation.

ACKNOWLEDGEMENTS

The authors wish to thank Dr R. D. Miller of IBM Almaden Research Center for providing the sample of PdnHS, and Dr K. Gardner for his advice, comments and help in obtaining the X-ray intensity data. The authors also gratefully acknowledge the continuing discussions and support of Dr J. F. Rabolt of IBM, who initiated this work while BLF was a visiting scientist in his laboratory. This work was supported, in part, by IBM under a co-operative research agreement.

REFERENCES

1 Kepler, R. G. *Synth. Met.* 1989, **28**, C573
2 Harrah, L. A. and Zeigler, J. M. *Macromolecules* 1987, **30**, 601
3 Zeigler, J. M. *Synth. Met.* 1989, **28**, C581
4 Miller, R. D. and Sooriyakumaran, R. *J. Polym. Sci., Polym. Chem. Edn* 1987, **25**, 111
5 Trefonas, P., Damewood, R., West, R. and Miller, R. D. *Organometallics* 1985, **4**, 1318
6 Miller, R. D., Hofer, D. and Fickes, G. N. *J. Am. Chem. Soc.* 1985, **107**, 2172
7 Rabolt, J. F., Song, K., Kuzmany, H., Sooriyakumaran, R., Fickes, G. and Miller, R. D. *Am. Chem. Soc., Polym. Prepr.* 1990, **31**, 262
8 Weber, P., Guillon, D., Skoulios, A. and Miller, R. D. *J. Phys. France* 1989, **50**, 793
9 Kuzmany, H., Rabolt, J. F., Farmer, B. L. and Miller, R. D. *J. Chem. Phys.* 1986, **85**, 7413
10 Lovinger, A. J., Schilling, F. C., Bovey, F. A. and Zeigler, J. M. *Macromolecules* 1986, **19**, 2657
11 Rabolt, J. F., Hofer, D., Miller, R. D. and Fickes, G. N. *Macromolecules* 1986, **19**, 611
12 Farmer, B. L., Rabolt, J. F. and Miller, R. D. *Macromolecules* 1987, **20**, 1167
13 Fraser, R. D. B., Macrae, T. P., Miller, A. and Rowlands, R. J. *J. Appl. Cryst.* 1976, **9**, 81
14 Fraser, R. D. B. and MacRae, T. P. 'Conformation in Fibrous Proteins', Academic Press, New York, 1973, p. 51
15 Patnaik, S. S., Farmer, B. L., Greso, A., Miller, R. D. and Rabolt, J. F. *Bull. Am. Phys. Soc.* 1990, **35**, 754
16 Smith, P. J. C. and Arnott, S. *Acta Cryst.* 1978, **A34**, 3
17 Chapman, B. R., Patnaik, S. S. and Farmer, B. L. *Am. Chem. Soc., Polym. Prepr.* 1990, **31**, 265
18 Stubbs, G. *Acta Cryst.* 1989, **A45**, 254
19 Millane, R. P. *Acta Cryst.* 1989, **A45**, 573
20 Alexander, L. E. 'X-ray Diffraction Methods in Polymer Science', Wiley-Interscience, New York, 1969
21 Varma-Nair, M., Cheng, J., Jin, Y. and Wunderlich, B. *Macromolecules* 1991, **24**, 5442
22 Fraser, R. D. B. and MacRae, T. P. 'Conformation in Fibrous Proteins', Academic Press, New York, 1973, p. 140
23 Plate, N. A., Shibaev, V. P., Petrukhin, B. S., Zubov, Yu. A. and Kargin, V. A. *J. Polym. Sci.* 1971, **9**, 2291
24 Hsieh, H. W. S., Post, B. and Morawetz, H. *J. Polym. Sci.* 1976, **14**, 1241
25 Hallmark, V. M., Sooriyakumaran, R., Miller, R. D. and Rabolt, J. F. *J. Chem. Phys.* 1989, **90**, 2486
26 Bryan, R. F. and Hartley, P. *Mol. Cryst. Liq. Cryst.* 1981, **69**, p. 47
27 Schilling, F. C., Bovey, F. A., Lovinger, A. and Zeigler, J. M. *Macromolecules* 1986, **19**, 2660
28 Gobbi, G. C., Fleming, W. W., Sooriyakumaran, R. and Miller, R. D. *J. Am. Chem. Soc.* 1986, **108**, 5624
29 Gomez, M. A., Tanaka, H. and Tonelli, A. E. *Polymer* 1987, **28**, 2227
30 Schilling, F. C., Bovey, F. A., Lovinger, A. J. and Zeigler, J. M. in 'Silicon-based Polymer Science' (Eds J. M. Zeigler and F. D. Gordon Fearon), American Chemical Society, Washington DC, 1990
31 VanderHart, D. L. *J. Magn. Reson.* 1981, **44**, 117
32 Greenberg, S. A. and Alfrey, T. *J. Am. Chem. Soc.* 1954, **76**, 6280
33 Wunderlich, B. 'Macromolecular Physics', Academic Press, New York, 1973, p. 88
34 Patnaik, S. S. and Farmer, B. L. *Polymer* in press